Reversible Data Hiding With Image Contrast Enhancement Based on Two-Dimensional Histogram Modification

HAO-TIAN WU[1], (Senior Member, IEEE), WEIQI MAI[1], SHUYI MENG[1], YIU-MING CHEUNG[2], (Fellow, IEEE), AND SHAOHUA TANG[1,3], (Member, IEEE)

[1]School of Computer Science and Engineering, South China University of Technology, Guangzhou 510006, China
[2]Department of Computer Science, Hong Kong Baptist University, Hong Kong
[3]Peng Cheng Laboratory, Shenzhen 518055, China.

Corresponding author: Yiu-Ming Cheung (ymc@comp.hkbu.edu.hk)

ABSTRACT Recently, reversible image data hiding with contrast enhancement (CE) has been proposed so that a contrast-changed image can be converted to its original version when needed. Several reversible image CE methods have been proposed by adopting the technique of reversible data hiding (RDH) to embed the recovery information into the contrast-enhanced images. In these methods, the 1D histogram is calculated and then modified to achieve the effects of histogram equalization (HE). Meanwhile, the 2D histogram has been used in image CE and demonstrated remarkable advantages in improving the image quality. In this paper, the method based on the 2D histogram modification is proposed to perform image CE and RDH simultaneously. In particular, a preprocessing strategy is developed to merge the adjacent bins in 2D histogram to prevent the overflow and underflow of the pixel values due to HE. The changes made in preprocessing is minimized by choosing the lowest bins for merging, while the CE effects can be achieved by expanding the highest bins for data embedding. The experimental results on two sets of test images have clearly demonstrated the efficacy of the proposed method for reversible image CE. The evaluation results are given to show its superior performances in CE and image quality preservation by comparing with the state-of-the-art approaches.

INDEX TERMS Image enhancement, reversible data hiding, 2D histogram, image quality.

I. INTRODUCTION

Contrast enhancement (CE) is a useful technique to improve the visibility of image content. For better interpretation of those images with limited dynamic range, CE is often performed to bring out unclear details. The technique of image CE has received much attention and been widely used in industrial and medical imagery (e.g., [1]–[5]). Among the methods have been proposed, one popular procedure is histogram equalization (HE) (e.g., [6], [7]).

A brief survey of the early image CE methods is presented in [8], where a HE based framework is proposed by

regarding CE as an optimization problem. In [9], a two-dimensional (2D) HE algorithm is proposed to utilize contextual information around each pixel to enhance the contrast of an input image. In [10], 2D histogram is further equalized for contextual and variational CE. Similarly, the gray-level differences between adjacent pixels are amplified in [11] by modifying the 2D histogram for CE. Moreover, saliency is preserved in automatic CE to prevent excessive enhancement in [12], while entropy measures calculated from the distribution of spatial locations of gray levels are used for CE in [13]. Entropy measures are also employed in the transform domain (e.g., [14]) to achieve both local and global CE effects. In [15], a general framework is proposed to accelerate the histogram-based image CE by selective down-sampling,
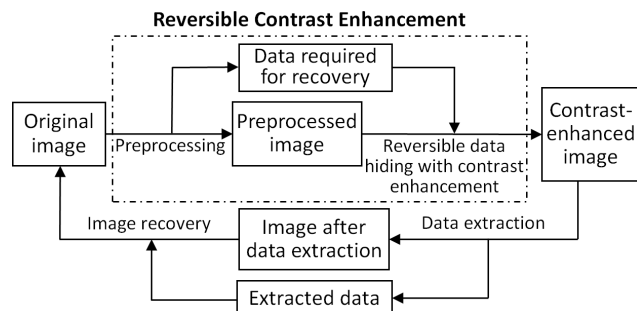
FIGURE 1. A flowchart of reversible image data hiding with contrast enhancement.

while two algorithms to detect the CE manipulations in digital images are further developed in [16].

As quite a lot of methods are developed for image CE, reversibility of image CE has been recently realized. In [17]–[25], several schemes have been proposed by using the technique of reversible data hiding (RDH) (e.g., [26]–[39]) to embed recovery information into the enhanced images. By performing image CE based on RDH, the effects of HE can be achieved during the process of data embedding. After that, the original image can be exactly recovered after extracting the hidden data. As shown in Figure 1, the original version of a contrast-changed image can be recovered without using any extra information. Such a property is appealing because image CE can be conducted without any information loss. In addition, extra data can be hidden into contrast-enhanced images to enable more functionalities such as authentication and annotation.

To the best of our knowledge, the first attempt to achieve HE effects by RDH was made in [17], where the highest two bins in one-dimensional (1D) histogram are chosen to be expanded into two adjacent bins for data embedding, respectively. By repeating the process of data embedding, the effects of HE can be achieved. But artificial distortions may be caused after conducting the preprocessing to prevent the overflows and underflows of pixel values due to bin expansion. To alleviate the visual distortions, an improved RDH method is proposed in [18] by setting an upper bound of the relative contrast error defined in [40]. Moreover, another RDH method is proposed for medical images in [19] to reduce the distortions introduced by preprocessing. In [20], an automatic CE method is proposed by using RDH. Moreover, RDH is conducted in medical images to enhance the contrast of texture area in [21]. In [22], image contrast is improved by making the histogram shifting process adaptive to the distribution characteristics. In addition, reversible CE of the region of interest and tamper localization for medical images are achieved in [23]. In [24], a new preprocessing strategy is proposed by preserving the orders of pixel values to achieve better visual quality. In [25], the algorithm proposed in [20] is equipped with brightness preservation so that better visual effects can be achieved.

To improve the performance in terms of the peaked signal-to-noise ratio (PSNR) value versus data hiding rate, RDH based on 2D histogram has been developed (e.g., [27]–[29]). However, reversible image CE based on 2D histogram has not been reported, though 2D histogram has been used in [9]–[11] and demonstrated remarkable advantages in improving image quality. Nevertheless, it is not an easy task to perform reversible image CE based on 2D histogram due to the following reasons. Firstly, as reported in [41], it is not accurate to measure the quality of contrast-enhanced images with PSNR, which is popularly used in performance evaluations of the conventional RDH methods. Secondly, the RDH methods proposed in [27]–[29] are performed in prediction value domain while the image CE schemes are developed in spatial domain. So directly applying them in the prediction error domain may not achieve satisfactory CE effects. Thirdly, preprocessing should be conducted on 2D histogram to avoid overflow or underflow of pixel values due to HE, but only 1D histogram is modified in the previous methods in [17]–[25].

To cope with these issues, a method for reversible image CE is proposed based on 2D histogram modification. To prevent overflow or underflow of pixel values due to HE, a new preprocessing is developed to shrink a 2D histogram. At each step, the adjacent rows/columns of bins in 2D histogram are merged, while the changes are minimized by choosing the lowest bins for merging. Meanwhile, the bookkeeping is generated to record the original values of those pixels contained in a merged bin. As a matter of fact, a bin in 1D histogram consists of a column and a row of bins in 2D histogram that correspond to the same pixel value. In the proposed preprocessing, a column is unnecessarily chosen with a row with the same pixel value so that generally less bookkeeping needs to be recorded. Similarly, the constraint on choosing the bins to be expanded for data embedding is also relaxed so that higher embedding rate can be achieved. We applied the proposed method on two sets of test images, and the obtained experimental results demonstrated its efficacy for reversible image CE. By comparing with the methods in [17], [19], [20], [24], the evaluation results on CE, reversible data hiding and image quality preservation are provided to show the performances of the proposed method.

The rest of this paper is organized as follows. In the next section, a new reversible image CE method based on 2D histogram modification will be presented. The experimental results on two sets of test images will be given in Section III, including the performance comparisons with the existing methods. Finally, we draw a conclusion in Section IV.

II. REVERSIBLE IMAGE CONTRAST ENHANCEMENT WITH A 2D HISTOGRAM

In this section, a new method is proposed for reversible image data hiding with CE based on 2D histogram modification. Firstly, the procedure of calculating a 2D histogram from an image to be enhanced is introduced. Then a preprocessing strategy is developed to shrink 2D histogram while the changes made in preprocessing are recorded by generated the bookkeeping. After that, a data embedding algorithm is
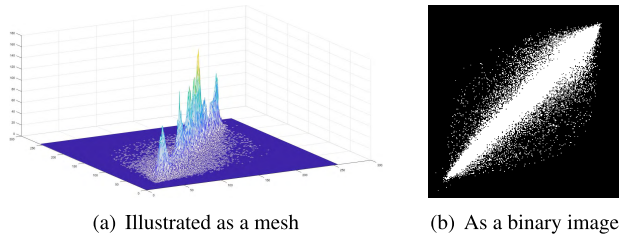
(a) Illustrated as a mesh   (b) As a binary image

FIGURE 2. A 2D histogram calculated from test image "Lena".

(a) Illustrated as a mesh   (b) As a binary image

FIGURE 3. A 2D histogram generated from the preprocessed image "Lena" by setting the margin width to 50.

presented to modify the preprocessed 2D histogram so that the bookkeeping and other necessary information required for original image recovery can be embedded. Finally, the procedure of converting a contrast-enhanced image to its original version is presented while the steps of implementing the proposed method are described in details.

A. GENERATING 2D HISTOGRAM FROM IMAGE

To calculate 1D histogram from a grayscale image, the occurrences of every possible pixel value are counted by scanning the image. To calculate 2D histogram, normally the occurrences of two adjacent pixel values are counted so that location information is taken into account. For instance, a pixel and the one to the right form a pair, and the non-overlapping pixel pairs in the image are scanned one by one. For a grayscale image, a 2D histogram $H = \{h(0, 0), \cdots, h(255, 255)\}$ is calculated after counting the number of each pair of pixel values, where $h(i, j)$ represents the number of pixel pairs with value (i, j) while $i \in \{0, \cdots, 255\}$ and $j \in \{0, \cdots, 255\}$. The 2D histogram calculated from test image "Lena" is illustrated in Figure 2 in two different ways. When illustrated as a mesh, the non-empty bins are visualized and the bin heights are plotted in the 2D plane. When illustrated as a binary image, only the locations of non-empty bins can be identified.

In such a 2D histogram, the pixel pairs contained in the same row of bins have the same pixel value on the right, while the pixel pairs contained in the same column of bins have the same pixel value on the left. Obviously, a bin in 1D histogram is equivalent to a column and a row of bins in 2D histogram with the same pixel value on the left or right of a pixel pair, respectively. In Figure 2, the non-empty histogram bins are roughly distributed along the diagonal, where the pixel pairs consisting of two identical values are contained, indicating that high correlations exist between the neighboring pixels.

B. PREPROCESSING

The purpose of preprocessing is to prevent the overflow and underflow of pixel values due to histogram shifting for HE. So a margin should be emptied along the boundary of 2D histogram, as shown in Figure 3 where the margin width is set to 50. To shrink a 2D histogram, it is natural to merge the adjacent rows and the adjacent columns. To minimize the changes made in bin merging, the row/column containing the lowest bin height (i.e., the sum
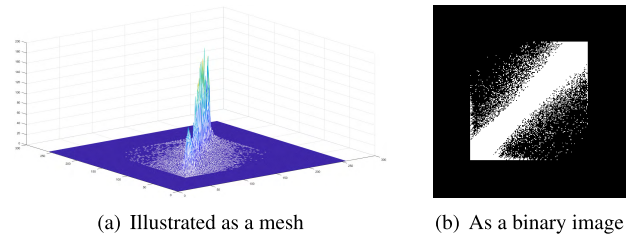

(a) Shifting in a 1D histogram   (b) Shifting in a 2D histogram
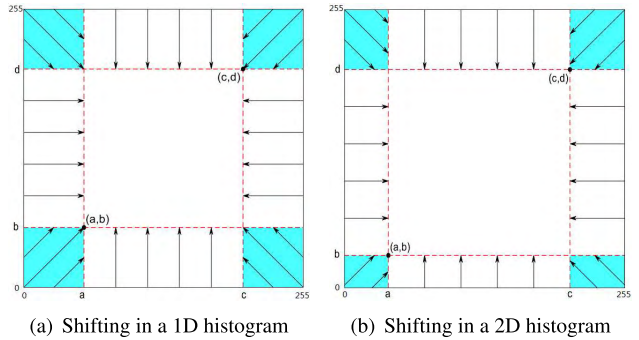
FIGURE 4. Histogram shifting directions in the proposed preprocessing.

of bin heights in the same row/column) is chosen to be merged with its adjacent row/column. By repeatedly merging the adjacent rows/columns for S times on each side of the 2D histogram, a margin with a width of S can be vacated around the non-empty bins. Meanwhile, the bookkeeping is generated to record the changes. A 2D histogram obtained from the preprocessed image "Lena" is illustrated in Figure 3.

As a bin in 1D histogram is equivalent to a column and a row in 2D histogram that correspond to the same pixel value, the preprocessing on 1D histogram (e.g., the one in [24]) is actually applied on the combination of a column and a row having intersection on the diagonal. With 2D histogram, the constraint is relaxed by separately choosing the columns and rows to be merged. As shown in Figure 4, the column corresponding to pixel value a is chosen to be merged with its adjacent column while the row corresponding to pixel value b is chosen to be merged with its adjacent row in preprocessing. Similarly, the column corresponding to pixel value c and the row corresponding to pixel value d are also chosen to be merging with the adjacent column/row. In the case of 1D histogram, a is equal to b while c is equal to d, as shown in Figure 4(a). With 2D histogram, a is unnecessarily equal to b and c is unnecessarily equal to d, as shown in Figure 4(b). To minimize the number of pixel pairs contained in the merged row/column, the row/column with the lowest bin height are separately chosen on each side of 2D histogram.

Now we introduce how to generate the bookkeeping to record the changes made in 2D histogram shrinkage. Suppose that column a contains the minimum number of pixel

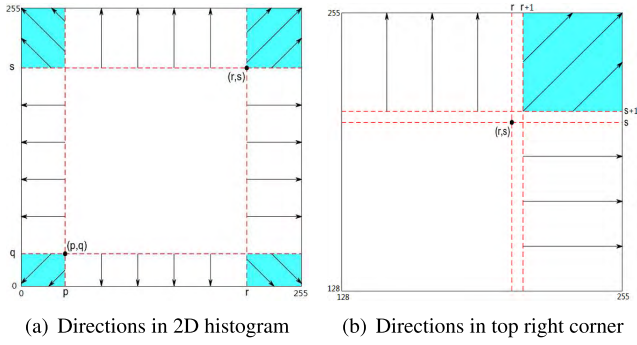(a) Directions in 2D histogram   (b) Directions in top right corner

FIGURE 5. Histogram equalization directions in the proposed method.

pairs among the columns with value less than 128, as shown in Figure 4(b). If there is no non-empty bins in column a, only the value a and a bit value 1 (indicating that column a is empty) need to be recorded. For those pixel pairs where the left pixel value is less than a, the left pixel value is added by 1 so that the empty column is shifted to the left of the non-empty columns. Otherwise, if there is at least one non-empty bin contained in column a, the value of a, a bit value 0 (indicating that column a is non-empty) and a string of bit values need to be recorded. The length of the string is equal to the number of pixel pairs contained in column a and column $a + 1$. By scanning all pixel pairs one by one, a bit value 1 is recorded for a pixel pair contained in column a while a bit value 0 is recorded for a pixel pair contained in column $a + 1$.

For pixel pairs contained in column a, the left pixel value is added by 1. The pixel pairs contained in column $a + 1$ are unchanged so that the two adjacent columns are merged. For pixel pairs where the left pixel value is less than a, the left pixel value is also added by 1 but no bit value needs to be recorded. As a result, an empty column is generated to the left of the non-empty columns. Similarly, column c and column $c - 1$, row b and row $b + 1$, row d and row $d - 1$, can be merged according to the directions as shown in Figure 4(b) to shift or generate an empty row/column to the right, below and above the non-empty columns/rows, respectively. By repeatedly merging the adjacent rows/columns for S times on each side of the 2D histogram, a margin with a width of S can be vacated around the non-empty bins. Then the generated bookkeeping is concatenated with its total length and the value of S, which are to be embedded during the process of CE for original image recovery.

C. DATA EMBEDDING WITH 2D HISTOGRAM

To perform data embedding, a row or a column of bins in 2D histogram are expanded at the same time. Specifically, a combination of the row and column with the maximum number of pixel pairs are chosen at each time. Suppose that column p, column r, row q and row s contain the maximum number of pixel pairs among those columns/rows less than 128 or larger than 127, as shown in Figure 5(a), where $p < r$ and $q < s$. For a pixel pair with value (i, j) contained in the

selected rows or columns, its value is modified to (i', j') for data embedding by

$$
(i', j') = \begin{cases}
(i + b_a, j + b_b), & \text{if } i = r \text{ and } j = s \\
(i - b_c, j + b_d), & \text{if } i = p \text{ and } j = s \\
(i - b_e, j - b_f), & \text{if } i = p \text{ and } j = q \\
(i + b_g, j - b_h), & \text{if } i = r \text{ and } j = q \\
(i + b_i, j + 1), & \text{if } i = r \text{ and } j > s \\
(i + b_j, j), & \text{if } i = r \text{ and } q < j < s \\
(i + b_k, j - 1), & \text{if } i = r \text{ and } j < q \\
(i - b_l, j + 1), & \text{if } i = p \text{ and } j > s \\
(i - b_m, j), & \text{if } i = p \text{ and } q < j < s \\
(i - b_n, j - 1), & \text{if } i = p \text{ and } j < q \\
(i + 1, j + b_o), & \text{if } j = s \text{ and } i > r \\
(i, j + b_p), & \text{if } j = s \text{ and } p < i < r \\
(i - 1, j + b_q), & \text{if } j = s \text{ and } i < p \\
(i + 1, j - b_r), & \text{if } j = q \text{ and } i > r \\
(i, j - b_s), & \text{if } j = q \text{ and } p < i < r \\
(i - 1, j - b_t), & \text{if } j = q \text{ and } i < p,
\end{cases}
\tag{1}
$$

where any of $\{b_a, b_b, \cdots, b_s, b_t\}$ is a bit value (0 or 1) to be embedded and its value varies according to the data stream to be hidden. As shown in Figure 5(b), any of the chosen rows/columns is expanded into two adjacent rows/columns. To prevent the expanded rows/columns from being overlapped with the surrounding rows/columns, those pixel pairs that are not included in the selected rows and columns are also modified by

$$
(i', j') = \begin{cases}
(i, j), & \text{if } p < i < r \text{ and } q < j < s \\
(i - 1, j), & \text{if } i < p \text{ and } q < j < s \\
(i + 1, j), & \text{if } i > r \text{ and } q < j < s \\
(i, j - 1), & \text{if } p < i < r \text{ and } j < q \\
(i, j + 1), & \text{if } p < i < r \text{ and } j > s \\
(i + 1, j + 1), & \text{if } i > r \text{ and } j > s \\
(i + 1, j - 1), & \text{if } i > r \text{ and } j < q \\
(i - 1, j + 1), & \text{if } i < p \text{ and } j > s \\
(i - 1, j - 1), & \text{if } i < p \text{ and } j < q.
\end{cases}
\tag{2}
$$

After processing all pixel pairs in the image, the non-empty bins are shifted toward the boundary of 2D histogram. The same process is repeated by expanding those rows/columns containing the maximum number of pixel pairs for S times in total. As a result, the histogram is spread over the 2D plane so that the effects of CE can be achieved with data embedding. Note that only one parameter (i.e., the margin width S) needs to be set for preprocessing and data embedding. Besides the information required for recovering the original image, extra data can be also hidden into the enhanced image.

D. DATA EXTRACTION AND IMAGE RECOVERY
Given that the values of those rows and columns that have been expanded in Figure 5 (e.g., $\{p, q, r, s\}$) are

provided, the histogram modification for data embedding can be reversed by modifying a pixel pair (i', j') back to

$$(i, j) = \begin{cases} (i', j'), & \text{if } p < i' < r \text{ and } q < j' < s \\ (r, s), & \text{in case 1} \\ (p, s), & \text{in case 2} \\ (p, q), & \text{in case 3} \\ (r, q), & \text{in case 4,} \end{cases} \quad (3)$$

where case 1 represents $i' \in \{r, r+1\}$ and $j' \in \{s, s+1\}$, case 2 represents $i' \in \{p-1, p\}$ and $j' \in \{s, s+1\}$, case 3 represents $i' \in \{p-1, p\}$ and $j' \in \{q, q-1\}$, while case 4 represents $i' \in \{r, r+1\}$ and $j' \in \{q, q-1\}$. In other cases, the original pixel pair (i, j) is equal to

$$\begin{cases} (r, j'-1), & \text{if } i' \in \{r, r+1\} \text{ and } j > s \\ (r, j'), & \text{if } i' \in \{r, r+1\} \text{ and } q < j < s \\ (r, j'+1), & \text{if } i' \in \{r, r+1\} \text{ and } j < q \\ (p, j'-1), & \text{if } i' \in \{p-1, p\} \text{ and } j > s \\ (p, j'), & \text{if } i' \in \{p-1, p\} \text{ and } q < j < s \\ (p, j'+1), & \text{if } i' \in \{p-1, p\} \text{ and } j < q \\ (i'-1, s), & \text{if } j' \in \{s, s+1\} \text{ and } i > r \\ (i', s), & \text{if } j' \in \{s, s+1\} \text{ and } p < i < r \\ (i'+1, s), & \text{if } j' \in \{s, s+1\} \text{ and } i < p \\ (i'-1, q), & \text{if } j' \in \{q-1, q\} \text{ and } i > r \\ (i', q), & \text{if } j' \in \{q-1, q\} \text{ and } p < i < r \\ (i'+1, q), & \text{if } j' \in \{q-1, q\} \text{ and } i < p \\ (i'-1, j'-1), & \text{if } i' > r+1 \text{ and } j' > s+1 \\ (i'+1, j'-1), & \text{if } i' < p-1 \text{ and } j' > s+1 \\ (i'+1, j'+1), & \text{if } i' < p-1 \text{ and } j' < q-1 \\ (i'-1, j'+1), & \text{if } i' > r+1 \text{ and } j' < q-1. \end{cases} \quad (4)$$

Furthermore, one or two bit values can be extracted by

$$\begin{cases} (i'-r, j'-s), & \text{in case 1} \\ (p-i', j'-s), & \text{in case 2} \\ (p-i', q-j'), & \text{in case 3} \\ (i'-r, q-j'), & \text{in case 4} \\ i'-r, & \text{if } i' \in \{r, r+1\}, j \neq q \text{ and } j \neq s \\ p-i', & \text{if } i' \in \{p-1, p\}, j \neq q \text{ and } j \neq s \\ j'-s, & \text{if } j' \in \{s, s+1\}, i \neq p \text{ and } i \neq r \\ q-j', & \text{if } j' \in \{q-1, q\}, i \neq p \text{ and } i \neq r. \end{cases} \quad (5)$$

With the extracted data, the side information required for data extraction and image recovery can be known, such as the value of S, the bookkeeping generated in preprocessing and its length. With the extracted value of S, Equation (3), (4) and (5) can be applied for the same time as applying Equation (1) and Equation (2) for data embedding. Eventually, the image after preprocessing can be obtained after extracting the data hidden in the contrast-enhanced image.

With the extracted bookkeeping, those bins that have been merged in pre-processing can be split. Given a pixel value a,

the corresponding row/column of bins in 2D histogram can be identified. In the case that a is less than 127, an empty row/column is created by shifting all the rows/columns less than $a + 1$ if the following bit value is 1. If the following bit value is 0, the rows/columns less than $a + 1$ are still shifted while the row/column $a + 1$ is split into two adjacent rows/columns. By scanning all pixel pairs in the image, the bit values in the bookkeeping are referred to when the right/left pixel value in a pair is equal to $a + 1$. If the corresponding bit value in the bookkeeping is 1, the right/left pixel value in a pair is subtracted by 1 to a. If the corresponding bit value in the bookkeeping is 0, the pixel pair is kept unchanged. In this way, the original image is recovered after splitting all bins merged in preprocessing according to the extracted bookkeeping.

E. DETAILED PROCEDURE OF PROPOSED METHOD

Suppose that a margin with width S needs to be vacated for an input image I. The **data embedding and contrast enhancement process** of the proposed method includes the following steps:

1) Generate a 2D histogram of I and globally shifting the histogram if its centroid is far from [127.5, 127.5];

2) Perform histogram shrinkage by merging the adjacent rows and columns on each side of 2D histogram as shown in Figure 4(b) for S times;

3) Generate the bookkeeping to record the bin merging information as described in Section II-B;

4) Perform data embedding by applying Equation (1) and Equation (2) for S-1 times to embed the global shifting information, the recorded bookkeeping and its length, etc.

5) Calculate a 2D histogram excluding the last 32 pixels (i.e., 16 pixel pairs) and expand the rows/columns containing the maximum number of pixel pairs on each side to embed the value of S, the least significant bits (LSB) of the last 32 pixels, and the previously expanded row/column values.

6) Replace the LSBs of the last 32 pixels with the lastly expanded row/column values (i.e., $\{p, q, r, s\}$ in Figure 5, where each value is represented with 8 bits) to generate the contrast-enhanced image I'.

The **data extraction and image recovery process** of the proposed method includes the following steps.

1) Collect the LSBs from the last 32 pixels in I' so as to know the lastly expanded row/column values;

2) Calculate a 2D histogram without counting the last 32 pixels and extract the hidden data by using (5) with the lastly expanded row/column values;

3) Obtain the value of S, the original LSB values of the 32 pixels, and the previously expanded row/column values from the extracted data and then apply Equation (3) and (4) to all pixel pairs contained in the histogram;

4) Write the original 32 LSB values back and calculate a 2D histogram from the whole image. Continue data extraction with the previously expanded row/column values by using Equation (3), (4) and (5) for S-1 times;

(a) Test image "Lena" (RCE=0.5, BRISQUE score: -4.43)

(b) Enhanced (S=20, embedded bits (pure): 89817, RCE=0.554, BRISQUE score: -2.79)

(c) Enhanced (S=30, embedded bits (pure): 125006, RCE=0.579, BRISQUE score: -2.26)

(d) Enhanced (S=40, embedded bits (pure): 134209, RCE=0.597, BRISQUE score: -1.23)

FIGURE 6. The original and contrast-enhanced (with the extra bits embedded) images of "Lena" after expanding 20, 30 and 40 rows or columns of bins on each side of the 2D histogram with the proposed method, respectively.

(a) Test image "Goldhill" (RCE=0.5, BRISQUE score: 9.04)

(b) Enhanced (S=20, embedded bits (pure): 125029, RCE=0.554, BRISQUE score: 10.31)

(c) Enhanced (S=30, embedded bits (pure): 167250, RCE=0.570, BRISQUE score: 9.49)

(d) Enhanced (S=40, embedded bits (pure): 202069, RCE=0.574, BRISQUE score: 8.73)

FIGURE 7. The original and contrast-enhanced (with the extra bits embedded) images of "Goldhill" after expanding 20, 30 and 40 rows or columns of bins on each side of the 2D histogram with the proposed method, respectively.

5) Reverse the preprocessing according to the extracted bookkeeping.

6) Use the extracted global shifting information (if any) to shift the whole 2D histogram to recover the original image.

III. EXPERIMENTAL RESULTS

In the experiments, 24 gray-level images converted from Kodak Lossless True Color Image Suite[1] and 8 gray-level images converted from USC-SIPI[2] were used for testing. The Kodak images are with the size of 768 × 512 or 512 × 768, which are popularly used for performance evaluation of image CE, while the USC-SIPI images are with the size of 512 × 512. Besides the necessary data for original image recovery, extra data consisting of close numbers of 0s and 1s were also embedded into the contrast-enhanced images.

A. PARAMETER SETTING

The sole parameter needs to be set in the proposed method is the margin width S, i.e., the time of expanding the rows or columns on each side of 2D histogram for data embedding. To preserve the content in the image to be enhanced, the maximum value of S is set to 64 in the proposed method. An integer within [2, 64] were set to S for the test images in the Kodak set and USC-SIPI set, respectively.

[1]URL: http://www.r0k.us/graphics/kodak/
[2]URL: http://sipi.usc.edu/database/

The experimental results show that the original images were exactly recovered from their contrast-enhanced images for a wide range of S value (i.e., [2, 64]). Besides the necessary data required for original image recovery, extra bits were embedded into the enhanced images, especially for a large value of S. For instance, the original and contrast-enhanced images of "Lena" and "Goldhill" with different S values are shown in Figure 6 and Figure 7, respectively.

B. METRICS FOR PERFORMANCE EVALUATION

From the contrast-enhanced images as shown in Figure 6 and Figure 7, it can be seen that CE effects were increased by expanding more bins in 2D histogram. In addition to visual inspection, several metrics were used to evaluate the CE effects, including the relative entropy error (REE), the relative mean brightness error (RMBE) and the relative contrast error (RCE) defined in [40], which were calculated between the original and contrast-enhanced images. Specifically, $RCE = 0.5$ when the image contrast is unchanged, while RCE>0.5 when the contrast has been enhanced. REE is within [0, 1] and REE>0.5 when image entropy has been increased. Unlike RCE and REE, RMBE=1 when image mean brightness is unchanged, while RMBE<1 in the case that the mean brightness has been changed.

Three image quality metrics including the Structural SIMilarity (SSIM) index [42], blind/referenceless image

TABLE 1. Statistical evaluation (mean) on 8 USC-SIPI images.

S	Method	RCE	REE	RMBE	BRISQUE	SSIM	PSNR (dB)	hiding rate
20	[17]	**0.548**	0.526	0.989	23.54	0.920	25.05	0.458
	[19]	0.547	0.525	0.989	23.41	0.927	25.09	0.451
	[20]	0.537	0.525	0.977	**22.19**	**0.943**	**26.43**	**0.482**
	[24]	0.543	0.526	0.987	22.74	0.936	25.54	0.452
	Proposed	0.545	**0.530**	**0.990**	22.64	0.932	25.45	0.447
30	[17]	**0.567**	0.533	0.983	27.89	0.852	21.72	**0.607**
	[19]	0.565	0.532	0.983	27.00	0.860	22.01	0.590
	[24]	0.555	0.533	0.980	23.48	**0.903**	**23.27**	0.582
	Proposed	0.561	**0.538**	**0.985**	**23.47**	0.893	22.94	0.581
40	[17]	**0.577**	0.535	**0.971**	34.89	0.755	19.27	**0.729**
	[19]	0.571	0.534	0.963	33.21	0.770	19.23	0.703
	[24]	0.565	0.537	0.971	**23.93**	**0.876**	**21.67**	0.658
	Proposed	0.573	**0.543**	0.970	24.25	0.856	20.97	0.667
50	[17]	0.581	0.537	0.966	44.38	0.647	17.28	**0.865**
	[19]	0.571	0.535	0.952	40.56	0.675	17.44	0.835
	[24]	0.572	0.538	**0.967**	**24.30**	**0.853**	**20.76**	0.676
	Proposed	**0.583**	**0.546**	0.962	24.69	0.822	19.69	0.700

TABLE 2. Statistical evaluation (mean) on 24 Kodak images.

S	Method	RCE	REE	RMBE	BRISQUE	SSIM	PSNR (dB)	hiding rate
20	[17]	**0.544**	0.528	**0.985**	16.65	0.902	24.89	0.511
	[19]	0.539	0.529	0.984	15.42	0.914	24.70	0.496
	[20]	0.541	0.532	0.966	14.01	0.915	23.37	**0.563**
	[24]	0.537	0.528	0.982	14.00	**0.928**	**25.02**	0.476
	Proposed	0.539	**0.534**	0.982	**13.79**	0.921	24.85	0.518
30	[17]	**0.560**	0.535	**0.976**	20.57	0.831	21.34	**0.695**
	[19]	0.555	0.535	0.975	19.84	0.843	21.53	0.655
	[24]	0.550	0.533	0.970	**15.08**	**0.890**	**22.27**	0.564
	Proposed	0.555	**0.541**	0.974	15.59	0.871	21.74	0.639
40	[17]	**0.572**	0.539	**0.966**	27.19	0.743	18.94	**0.847**
	[19]	0.569	0.539	0.966	26.37	0.755	19.12	0.800
	[24]	0.559	0.535	0.962	**16.13**	**0.865**	**20.88**	0.603
	Proposed	0.570	**0.546**	0.964	16.49	0.825	19.68	0.715
50	[17]	**0.581**	0.542	**0.954**	35.93	0.638	16.76	**0.986**
	[19]	0.578	0.541	0.952	34.71	0.653	16.98	0.954
	Proposed	0.580	**0.549**	0.951	**17.42**	**0.797**	**18.36**	0.763

spatial quality evaluator (BRISQUE) [43] and Peaked Signal-to-Noise Ratio (PSNR) were calculated from the enhanced images, respectively. The reason to include the no-reference BRISQUE is due to that PSNR and SSIM are not very suitable for image quality assessment in the scenario of CE. Similar to most of the no-reference image quality evaluation methodologies (e.g., [44]), the BRISQUE scores typically have a value between 0 and 100 (0 represents the best quality, while 100 represents the worst), while the scores may be lower than 0 for images with good quality. Since extra bits were embedded into the contrast-enhanced images, pure hiding rate was calculated by subtracting the amount of data recorded for original image recovery from the total amount of embedded data and then divided by the total pixel number. Thus the pure hiding rate is represented in bit per pixel (bpp in short).

C. STATISTICAL PERFORMANCE COMPARISONS

To compare the CE effects, the RCE, REE and RMBE values obtained on two image sets with the proposed method were compared with those obtained with [17], [19], [20], [24]. In the experiments, several values (i.e., 20, 30, 40 and 50) were assigned to S in applying the five methods, respectively. The statistical results calculated from the enhanced images were listed in Table 1 and Table 2, where each item is the mean of 8 or 24 test images, respectively. The evaluation results obtained with the same value of S were listed in the same row. In applying [20], only the case of S = 20 were applicable to all test images while the other cases (i.e., S = 30, S = 40 and S = 50) could not be applied to all images in the two sets. Similarly, the method in [24] could not be applied to all images in the Kodak set with S = 50. From the statistical results, it can be seen that the effects of contrast enhancement (represented by RCE and REE) were increased by expanding more histogram bins. The hiding rate was also increased when more histogram bins were expanded. Meanwhile, the BRISQUE scores were more or less increased, while the RMBE, SSIM and PSNR values

were all decreased, showing that the differences between the original and contrast-enhanced images were enlarged.

From the RCE values listed in the two tables, it can be seen that the most CE effects were obtained by applying the method in [17] with $S = 20$, $S = 30$ and $S = 40$, respectively. However, the image quality obtained with the method in [17] was the worst (reflected by the lowest SSIM, PSNR values and the highest BRISQUE scores). Meanwhile, comparable RCE values were obtained with the proposed method (especially when S = 50 for the USC-SIPI set), which were always higher than those obtained with the method in [24] for all cases of S and different image sets. Moreover, the highest REE values were always obtained with the proposed method, indicating that the most information gain was achieved.

For the both image sets, the highest pure hiding rate was obtained with the method in [20] when S = 20 while the one obtained with the method in [17] was the highest in the case of S = 30, S = 40 and S = 50. With the proposed method, the rows and columns of bins could be separately chosen to achieve the highest hiding rate. For exchange, the values of the merged or expanded rows and columns should be recorded, which were more than those recorded when applying the methods using 1D histogram. As more histogram bins were used for data embedding, less pure hiding rate was obtained with the proposed method than those in [17], [19]. Nevertheless, much better image quality (represented by BRISQUE, SSIM and REE) was achieved with the proposed method than that obtained with [17], [19].

D. PERFORMANCES ON INDIVIDUAL IMAGES

To further evaluate the performances of the proposed method, the experimental results obtained on individual images were collected and compared with those obtained by applying the methods in [17], [19], [20], [24], respectively. As reported in [41], quality of the contrast-enhanced images can be better measured with the no-reference metric BRISQUE than PSNR and SSIM. So the BRISQUE scores were calculated from the enhanced images of "Baboon", "F-16",

(a) Results on test image "Baboon" (b) Results on test image "F-16" (c) Results on test image "Goldhill" (d) Results on test image "Lena"
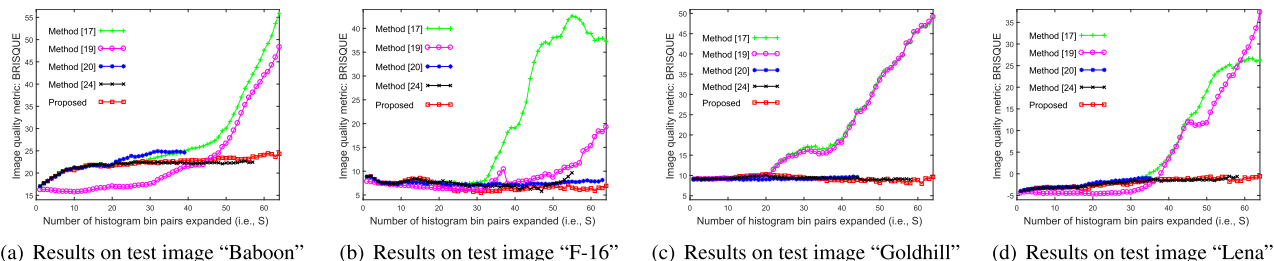
FIGURE 8. The BRISQUE scores with respect to *S* on four USC-SIPI image by applying the proposed and the methods in [17], [19], [20], [24], respectively.

(a) Results on test image "Baboon" (b) Results on test image "F-16" (c) Results on test image "Goldhill" (d) Results on test image "Lena"
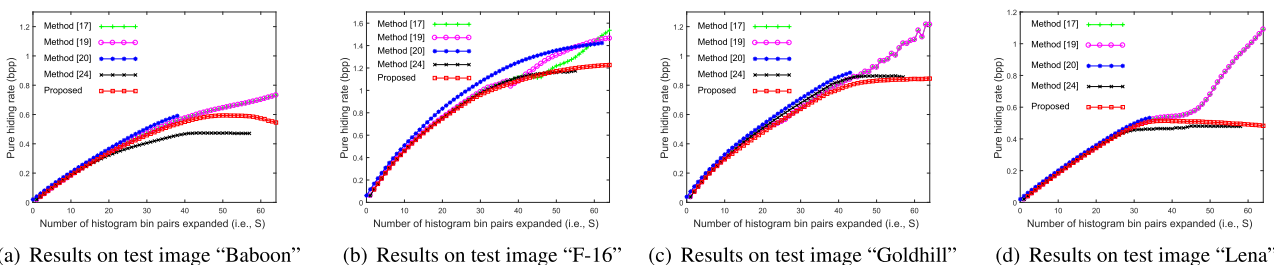
FIGURE 9. The pure data hiding rates with respect to *S* on four USC-SIPI image by applying the proposed and the methods in [17], [19], [20], [24], respectively.
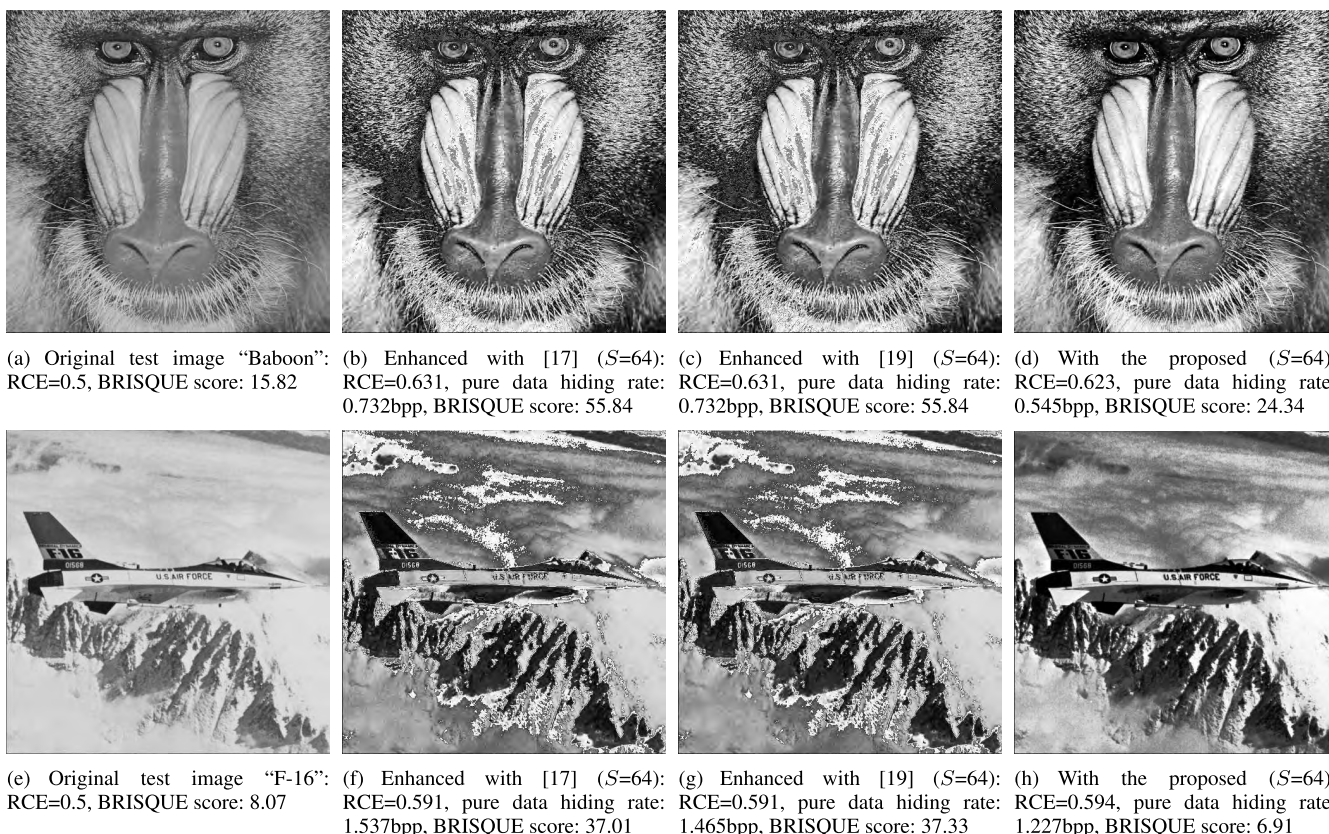

(a) Original test image "Baboon": RCE=0.5, BRISQUE score: 15.82

(b) Enhanced with [17] (*S*=64): RCE=0.631, pure data hiding rate: 0.732bpp, BRISQUE score: 55.84

(c) Enhanced with [19] (*S*=64): RCE=0.631, pure data hiding rate: 0.732bpp, BRISQUE score: 55.84

(d) With the proposed (*S*=64): RCE=0.623, pure data hiding rate: 0.545bpp, BRISQUE score: 24.34

(e) Original test image "F-16": RCE=0.5, BRISQUE score: 8.07

(f) Enhanced with [17] (*S*=64): RCE=0.591, pure data hiding rate: 1.537bpp, BRISQUE score: 37.01

(g) Enhanced with [19] (*S*=64): RCE=0.591, pure data hiding rate: 1.465bpp, BRISQUE score: 37.33

(h) With the proposed (*S*=64): RCE=0.594, pure data hiding rate: 1.227bpp, BRISQUE score: 6.91

FIGURE 10. The original and contrast-enhanced images by applying the proposed and the methods in [17], [19], respectively.

"Goldhill" and "Lena", which were generated by assigning the integers within $[2, 64]$ to *S*, respectively. Then the BRISQUE scores were plotted with respect to *S* for each

of the four USC-SIPI images to obtain the figures as shown in Figure 8, respectively. In Figure 8, there are five curves in each figure and each curve is corresponding to a reversible
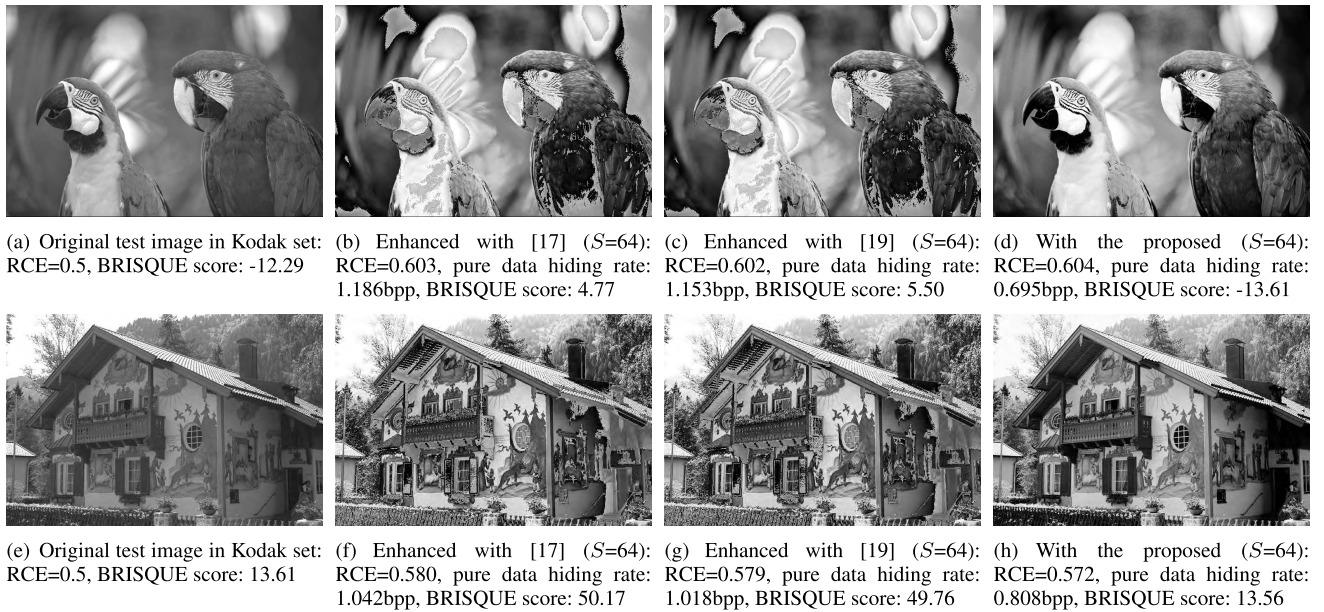
(a) Original test image in Kodak set: RCE=0.5, BRISQUE score: -12.29

(b) Enhanced with [17] (S=64): RCE=0.603, pure data hiding rate: 1.186bpp, BRISQUE score: 4.77

(c) Enhanced with [19] (S=64): RCE=0.602, pure data hiding rate: 1.153bpp, BRISQUE score: 5.50

(d) With the proposed (S=64): RCE=0.604, pure data hiding rate: 0.695bpp, BRISQUE score: -13.61

(e) Original test image in Kodak set: RCE=0.5, BRISQUE score: 13.61

(f) Enhanced with [17] (S=64): RCE=0.580, pure data hiding rate: 1.042bpp, BRISQUE score: 50.17

(g) Enhanced with [19] (S=64): RCE=0.579, pure data hiding rate: 1.018bpp, BRISQUE score: 49.76

(h) With the proposed (S=64): RCE=0.572, pure data hiding rate: 0.808bpp, BRISQUE score: 13.56

FIGURE 11. The original and contrast-enhanced images by applying the proposed and the methods in [17], [19], respectively.

image CE method applied to the test image. A curve consists of at most 63 BRISQUE scores and each value represents an image enhanced by applying the same method with a specified S value. Since the range of S is usually limited when applying the method in [20], the corresponding curves are shorter than those obtained with the other methods except for "F-16".

Different from the curve of PSNR versus data hiding rate in evaluating the traditional RDH methods (e.g., [27]–[39]), the BRISQUE curves should be as low as possible for a smaller BRISQUE score represents better image quality. In some cases, image quality did not become worse after being enhanced with the proposed method so that the corresponding curves slightly go down. Among all of the methods compared, the curves corresponding to the proposed method are always among the lowest ones for $S \in [2, 64]$. For the methods in [17], [19], the BRISQUE curves rapidly rise as the value of S is increased, indicating that visual distortions were introduced to the enhanced images. So the proposed method and [20], [24] performed better than [17], [19] for all of the four test images. The three BRISQUE curves obtained with the methods in [20], [24] and the proposed one in each figure are close when the value of S is small, but larger values could be assigned to S in applying the proposed method. Hence, the proposed method is most stable to achieve satisfactory quality of the enhanced images by adopting 2D histogram.

In Figure 9, the pure hiding rate is illustrated with respect to S for the four test images, respectively. Similar to Figure 8, there are five curves in each figure and each curve is corresponding to a specific method. Generally speaking, the obtained pure hiding rates were increased by expanding more histogram bins for data embedding. Moreover,

the hiding rates obtained with the methods in [17], [19] were generally higher when S is close to 64. This is because the JBIG2 compression [45] is adopted in [17], [19] while the bookkeeping is generated in [20], [24] and the proposed method (e.g., the pixel value corresponding to every row or column that is merged in preprocessing and expanded for data embedding). When applying the method in [20], the bookkeeping cannot be pre-calculated so that the embedding capacity is limited except for "F-16" among the four test images.

Although high hiding rates were also obtained with the methods in [17], [19], obvious visual distortions were caused when the value of S was increased. By applying the proposed method with $S = 64$, there is no such distortion in the contrast-enhanced images, as shown in Figure 10 and Figure 11, respectively for test images in USC-SIPI set and Kodak set. As comparable CE effects (represented by the RCE and REE values) were obtained with better image quality, generally better performances were achieved with the proposed method based on 2D histogram modification.

IV. CONCLUSION

In this paper, we have proposed a new reversible data hiding method with image contrast enhancement. A preprocessing strategy has been developed by merging the adjacent rows or columns of bins in two-dimensional histogram while the changes that have been made can be recorded. Since the constraints on choosing the bins have been relaxed in two-dimensional plane, the lowest bins are chosen in preprocessing while the highest bins can be expanded for data embedding. Thus comparable contrast enhancement effects can be obtained with satisfactory image quality.

Different from the normal methods, the process of image contrast enhancement can be performed in a lossless manner with the proposed method. The experimental results on two image sets have shown that an original image can be exactly recovered from a series of its contrast-enhanced versions. Moreover, the degree of contrast enhancement can be adjusted with respect to only one parameter. Compared with the methods using one-dimensional histogram, generally better performances in contrast enhancement effects and image quality have been achieved based on two-dimensional histogram modification.

REFERENCES

[1] S. Cakir, D. C. Kahraman, R. Cetin-Atalay, and A. E. Cetin, "Contrast enhancement of microscopy images using image phase information," *IEEE Access*, vol. 6, pp. 3839–3850, 2018.

[2] S. Park, S. Yu, M. Kim, K. Park, and J. Paik, "Dual autoencoder network for retinex-based low-light image enhancement," *IEEE Access*, vol. 6, pp. 22084–22093, 2018.

[3] S. Li, W. Jin, X. Wang, L. Li, and M. Liu, "Contrast enhancement algorithm for outdoor infrared images based on local gradient-grayscale statistical feature," *IEEE Access*, vol. 6, pp. 57341–57352, 2018.

[4] K. Lee, J. Lee, J. Lee, S. Hwang, and S. Lee, "Brightness-based convolutional neural network for thermal image enhancement," *IEEE Access*, vol. 5, pp. 26867–26879, 2017.

[5] Y. Guo, X. Ke, J. Ma, and J. Zhang, "A pipeline neural network for low-light image enhancement," *IEEE Access*, vol. 7, pp. 13737–13744, 2019.

[6] J. A. Stark, "Adaptive image contrast enhancement using generalizations of histogram equalization," *IEEE Trans. Image Process.*, vol. 9, no. 5, pp. 889–896, May 2000.

[7] J.-Y. Kim, L.-S. Kim, and S.-H. Hwang, "An advanced contrast enhancement using partially overlapped sub-block histogram equalization," *IEEE Trans. Circuits Syst. Video Technol.*, vol. 11, no. 4, pp. 475–484, Apr. 2001.

[8] T. Arici, S. Dikbas, and Y. Altunbasak, "A histogram modification framework and its application for image contrast enhancement," *IEEE Trans. Image Process.*, vol. 18, no. 9, pp. 1921–1935, Sep. 2009.

[9] T. Celik, "Two-dimensional histogram equalization and contrast enhancement," *Pattern Recognit.*, vol. 45, no. 10, pp. 3810–3824, Oct. 2012.

[10] T. Celik and T. Tjahjadi, "Contextual and variational contrast enhancement," *IEEE Trans. Image Process.*, vol. 20, no. 12, pp. 3431–3441, Dec. 2011.

[11] C. Lee, C. Lee, and C.-S. Kim, "Contrast enhancement based on layered difference representation of 2D histograms," *IEEE Trans. Image Process.*, vol. 22, no. 12, pp. 5372–5384, Dec. 2013.

[12] K. Gu, G. Zhai, X. Yang, W. Zhang, and C. W. Chen, "Automatic contrast enhancement technology with saliency preservation," *IEEE Trans. Circuits Syst. Video Technol.*, vol. 25, no. 9, pp. 1480–1494, Sep. 2015.

[13] T. Celik, "Spatial entropy-based global and local image contrast enhancement," *IEEE Trans. Image Process.*, vol. 23, no. 12, pp. 5298–5308, Dec. 2014.

[14] S. S. Agaian, B. Silver, and K. A. Panetta, "Transform coefficient histogram-based image enhancement algorithms using contrast entropy," *IEEE Trans. Image Process.*, vol. 16, no. 3, pp. 741–758, Mar. 2007.

[15] G. Cao, H. Tian, L. Yu, X. Huang, and Y. Wang, "Acceleration of histogram-based contrast enhancement via selective downsampling," *IET Image Process.*, vol. 12, no. 3, pp. 447–452, 2018.

[16] G. Cao, Y. Zhao, R. Ni, and X. Li, "Contrast enhancement-based forensics in digital images," *IEEE Trans. Inf. Forensics Security*, vol. 9, no. 3, pp. 515–525, Mar. 2014.

[17] H.-T. Wu, J.-L. Dugelay, and Y.-Q. Shi, "Reversible image data hiding with contrast enhancement," *IEEE Signal Process. Lett.*, vol. 22, no. 1, pp. 81–85, Jan. 2015.

[18] G. Gao and Y.-Q. Shi, "Reversible data hiding using controlled contrast enhancement and integer wavelet transform," *IEEE Signal Process. Lett.*, vol. 22, no. 11, pp. 2078–2082, Nov. 2015.

[19] H.-T. Wu, J. Huang, and Y.-Q. Shi, "A reversible data hiding method with contrast enhancement for medical images," *J. Vis. Commun. Image Represent.*, vol. 31, pp. 146–153, Aug. 2015.

[20] S. Kim, R. Lussi, X. Qu, and H. J. Kim, "Automatic contrast enhancement using reversible data hiding," in *Proc. IEEE Int. Workshop Inf. Forensics Secur.*, Nov. 2015, pp. 1–5.

[21] Y. Yang, W. Zhang, D. Liang, and N. Yu, "Reversible data hiding in medical images with enhanced contrast in texture area," *Digit. Signal Process.*, vol. 52, pp. 13–24, May 2016.

[22] H. Chen, J. Ni, W. Hong, and T.-S. Chen, "Reversible data hiding with contrast enhancement using adaptive histogram shifting and pixel value ordering," *Signal Process., Image Commun.*, vol. 46, pp. 1–16, Aug. 2016.

[23] G. Gao, X. Wan, S. Yao, Z. Cui, C. Zhou, and X. Sun, "Reversible data hiding with contrast enhancement and tamper localization for medical images," *Inf. Sci.*, vols. 385–386, pp. 250–265, Apr. 2017.

[24] H.-T. Wu, S. Tang, J. Huang, and Y.-Q. Shi, "A novel reversible data hiding method with image contrast enhancement," *Signal Process., Image Commun.*, vol. 62, pp. 64–73, Mar. 2018.

[25] S. Kim, R. Lussi, X. Qu, F. Huang, and H. J. Kim, "Reversible data hiding with automatic brightness preserving contrast enhancement," *IEEE Trans. Circuits Syst. Video Technol.*, to be published. doi: 10.1109/TCSVT.2018.2869935.

[26] Y.-Q. Shi, X. Li, X. Zhang, H.-T. Wu, and B. Ma, "Reversible data hiding: Advances in the past two decades," *IEEE Access*, vol. 4, pp. 3210–3237, 2016.

[27] B. Ou, X. Li, Y. Zhao, R. Ni, and Y.-Q. Shi, "Pairwise prediction-error expansion for efficient reversible data hiding," *IEEE Trans. Image Process.*, vol. 22, no. 12, pp. 5010–5021, Dec. 2013.

[28] X. Li, W. Zhang, X. Gui, and B. Yang, "A novel reversible data hiding scheme based on two-dimensional difference-histogram modification," *IEEE Trans. Inf. Forensics Security*, vol. 8, no. 7, pp. 1091–1100, Jul. 2013.

[29] I.-C. Dragoi and D. Coltuc, "Adaptive pairing reversible watermarking," *IEEE Trans. Image Process.*, vol. 25, no. 5, pp. 2420–2422, May 2016.

[30] Y. M. Cheung and H. T. Wu, "A sequential quantization strategy for data embedding and integrity verification," *IEEE Trans. Circuits Syst. Video Technol.*, vol. 17, no. 8, pp. 1007–1016, Aug. 2007.

[31] H.-T. Wu and Y.-M. Cheung, "Reversible watermarking by modulation and security enhancement," *IEEE Trans. Instrum. Meas.*, vol. 59, no. 1, pp. 221–228, Jan. 2010.

[32] X. Li, B. Yang, and T. Zeng, "Efficient reversible watermarking based on adaptive prediction-error expansion and pixel selection," *IEEE Trans. Image Process.*, vol. 20, no. 12, pp. 3524–3533, Dec. 2011.

[33] H.-T. Wu and J. Huang, "Reversible image watermarking on prediction errors by efficient histogram modification," *Signal Process.*, vol. 92, no. 12, pp. 3000–3009, Dec. 2012.

[34] X. Wu and W. Sun, "High-capacity reversible data hiding in encrypted images by prediction error," *Signal Process.*, vol. 104, pp. 387–400, Nov. 2014.

[35] I. C. Dragoi and D. Coltuc, "On local prediction based reversible watermarking," *IEEE Trans. Image Process.*, vol. 24, no. 4, pp. 1244–1246, Apr. 2015.

[36] X. Li, W. Zhang, X. Gui, and B. Yang, "Efficient reversible data hiding based on multiple histograms modification," *IEEE Trans. Inf. Forensics Security*, vol. 10, no. 9, pp. 2016–2027, Sep. 2015.

[37] W. Zhang, H. Wang, D. Hou, and N. Yu, "Reversible data hiding in encrypted images by reversible image transformation," *IEEE Trans. Multimedia*, vol. 18, no. 8, pp. 1469–1479, Aug. 2016.

[38] J. Wang, X. Chen, J. Ni, N. Mao, and Y. Shi, "Multiple histograms based reversible data hiding: Framework and realization," *IEEE Trans. Circuits Syst. Video Technol.*, to be published. doi: 10.1109/TCSVT.2019.2915584.

[39] J. Wang, N. Mao, X. Chen, J. Ni, C. Wang, and Y. Shi, "Multiple histograms based reversible data hiding by using FCM clustering," *Signal Process.*, vol. 159, pp. 193–203, Jun. 2019.

[40] M.-Z. Gao, Z.-G. Wu, and L. Wang, "Comprehensive evaluation for HE based contrast enhancement techniques," in *Advances in Intelligent Systems and Applications*, vol. 2. Berlin, Germany: Springer, 2013, pp. 331–338.

[41] H.-T. Wu, S. Tang, and Y.-Q. Shi, "Image quality assessment in reversible data hiding with contrast enhancement," in *Proc. 16th Int. Workshop Digit.-Forensics Watermarking (IWDW)*, in Lecture Notes in Computer Science, Magdeburg, Germany, vol. 10431, Aug. 2017, pp. 290–302.

[42] Z. Wang, A. C. Bovik, H. R. Sheikh, and E. P. Simoncelli, "Image quality assessment: From error visibility to structural similarity," *IEEE Trans. Image Process.*, vol. 13, no. 4, pp. 600–612, Apr. 2004.

[43] A. Mittal, A. K. Moorthy, and A. C. Bovik, "No-reference image quality assessment in the spatial domain," *IEEE Trans. Image Process.*, vol. 21, no. 12, pp. 4695–4708, Dec. 2012.

[44] A. K. Moorthy and A. C. Bovik, "Blind image quality assessment: From natural scene statistics to perceptual quality," *IEEE Trans. Image Process.*, vol. 20, no. 12, pp. 3350–3364, Dec. 2011.

[45] P. G. Howard, F. Kossentini, B. Martins, S. Forchhammer, and W. J. Rucklidge, "The emerging JBIG2 standard," *IEEE Trans. Circuits Syst. Video Technol.*, vol. 8, no. 7, pp. 838–848, Nov. 1998.

HAO-TIAN WU (SM'15) received the Ph.D. degree from the Department of Computer Science, Hong Kong Baptist University, Hong Kong, in 2007. From 2008 to 2009, he was a Postdoctoral Research Engineer with EURECOM, France. In 2013, he was a Visiting Scholar with the Computer Science and Engineering Department, New York University Tandon School of Engineering, for one year. He is currently an Associate Professor with the School of Computer Science and Engineering, South China University of Technology, Guangzhou, China. His research interests include information hiding, cyber space security, image and video processing, and signal processing in the encrypted domain. He is also a member of the IEEE Signal Processing Society and has been invited as a reviewer for several international journals and conferences.

WEIQI MAI is currently pursuing the bachelor's degree in information security with the School of Computer Science and Engineering, South China University of Technology, Guangzhou, China. His research interests include image processing and reversible data hiding.

SHUYI MENG is currently pursuing the bachelor's degree in information security with the School of Computer Science and Engineering, South China University of Technology, Guangzhou, China. His research interests include reversible data hiding and machine learning.

YIU-MING CHEUNG (SM'06–F'18) received the Ph.D. degree from the Department of Computer Science and Engineering, The Chinese University of Hong Kong, Hong Kong. He is currently a Full Professor with the Department of Computer Science, Hong Kong Baptist University, Hong Kong. His current research interests include machine learning, pattern recognition, visual computing, and optimization. He is an IET Fellow, a BCS Fellow, an RSA Fellow, and a Distinguished Fellow of the IETI. He also serves as an Associate Editor for the IEEE Transactions on Neural Networks and Learning Systems, IEEE Transactions on Cybernetics, *Pattern Recognition*, and *Neurocomputing*, to name a few.

SHAOHUA TANG (M'99) received the B.Sc. and M.Sc. degrees in applied mathematics and the Ph.D. degree in communication and information system from the South China University of Technology, China, in 1991, 1994, and 1998, respectively. He was a Visiting Scholar with North Carolina State University and the University of Cincinnati, USA. He has been a Full Professor with the School of Computer Science and Engineering, South China University of Technology, since 2004. He is also a jointly appointed Full Professor with the Peng Cheng Laboratory, Shenzhen, China. He has authored or coauthored over 100 technical papers in journals and conference proceedings. His current research interests include information security, data security, and privacy preserving in cloud computing and big data. He is also a member of the IEEE Computer Society.

• • •